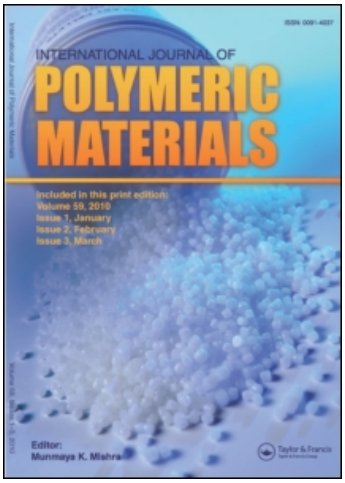

International Journal of Polymeric Materials
Publication details, including instructions for authors and subscription information:
http://www.informaworld.com/smpp/title~content=t713647664

Dielectric Spectroscopy of Conducting Polyaniline Polymer

H. M. El Ghanem[a]; H. Attar[b]; H. Sayid Ahmad[b]; S. Abduljawad[c]
[a] Physics Department, Jordan University of Science and Technology, Irbid, Jordan [b] Physics Department, Al-Bayt University, Al Mafraq, Jordan [c] Physics Department, Hashemite University, Zarqa, Jordan

To cite this Article Ghanem, H. M. El , Attar, H. , Ahmad, H. Sayid and Abduljawad, S.(2006) 'Dielectric Spectroscopy of Conducting Polyaniline Polymer', International Journal of Polymeric Materials, 55: 9, 663 — 679
To link to this Article: DOI: 10.1080/00914030500323318
URL: http://dx.doi.org/10.1080/00914030500323318

International Journal of Polymeric Materials, 55:663–679, 2006

ISSN: 0091-4037 print/1563-5333 online
DOI: 10.1080/00914030500323318

Taylor & Francis
Taylor & Francis Group

Dielectric Spectroscopy of Conducting Polyaniline Polymer

H. M. El Ghanem
Physics Department, Jordan University of Science and Technology, Irbid, Jordan

H. Attar
H. Sayid Ahmad
Physics Department, Al-Bayt University, Al Mafraq, Jordan

S. Abduljawad
Physics Department, Hashemite University, Zarqa, Jordan

The dielectric spectroscopy of conducting polyaniline polymers (PANI) in the form of emeraldine base and emeraldine salt was carried out in the temperature range 30 to 80°C and in the frequency range 1 Hz to 1 MHz. The imaginary part of the impedance (Z″) versus frequency exhibits a relaxation peak , the positions of the peaks are shifted toward lower frequencies for concentrations below 0.1 M, whereas the peaks are shifted to higher frequencies for concentrations above 0.1 M. The PANI samples were protonated (doped) externally with various concentrations of aqueous sulfuric acid in the range of 0.05 to 0.2 molar. The thermal behavior of undoped and doped PANI samples has been analyzed, using thermal gravimetric analysis and differential scanning calorimetry techniques, and reveal that transition in the thermal behavior has been observed for concentrations above 0.1 molar. The a.c. conductivity measurements reveal that insulator to metal transition in the conductivity of these samples was observed for acid concentration greater than 0.1 molar. The a.c. conductivity for the protonated samples bellow 0.1 molar follows an Arrhenius behavior $\partial\sigma/\partial T < 0$ *with two activation energies, while* $\partial\sigma/\partial T > 0$ *for acid concentration greater than 0.1 M.*

Keywords: conductivity, dielectric constant conducting polymers, polyaniline

Received 16 July 2005; in final form 15 August 2005.

One of the authors (H. M. El Ghanem) wishes to thank Jordan University of Science and Technology for financial support.

Address correspondence to S. Abduljawad, Physics Department, Faculty of Sciences and Arts, Hashemite University, P. O. Box 150459, Zarqa 13115, Jordan. E-mail: saadi@hu.edu.jo

INTRODUCTION

Polyaniline (PANI) exists in a variety of forms that differ in chemical and physical properties [1–4]. The physical properties depend mainly on the process of preparation used. The most common nonconducting blue emeraldine base is an insulator, while the protonated emeraldine salt, shown in Figure 1, generally has a green color and has conductivity on the semiconductor level, many orders of magnitude higher than that of common polymers.

The changes in the physicochemical properties of PANI occurring as a response to an external stimuli are used in various applications [5–6], for example, in organic electrodes, sensors, and actuators [7–9]. Other uses are based on the combination of electrical properties typical of semiconductors with materials parameters characteristic of polymers, like the development of plastic microelectronics [10], electrochromic devices [11], tailor-made composite systems [12–13], and smart fabrics [14]. The potential applications of PANI depend heavily on method of preparation, type, and concentration of the acid used.

It has been reported [15] that the macromolecular and supramolecular structures of PANI are controlled by the reaction conditions. So, it is of obvious interest for the design of applications to learn how these structural features are related to the electrical properties of a conducting polymer. The DC conduction of polyaniline has been well studied by several authors [16–20] and several mechanisms have

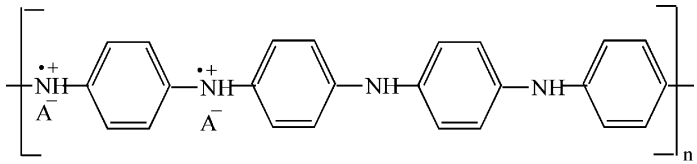

Polyaniline (emeraldine) salt

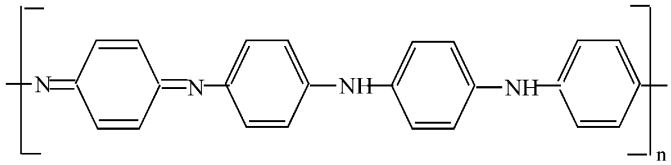

Polyaniline (emeraldine) base

FIGURE 1 PANI structure.

been proposed to explain electric conduction in polymers. Kivelson [21] was the first to use the inter-soliton hopping model. Other models like electron hopping and dipolar relaxation have been used to explain the dielectric data of PANI salts. But it seems that no definite theory exists to explain the origin of electric conduction or the reported near metal insulator transition occurs in conducting PANI.

It is the purpose of this article to further investigate the effect of concentration and method of preparation on the dielectric properties of PANI, and to study the origin of electric conduction by measuring the low frequency conductivity and dielectric relaxation in order to provide additional information on the mechanism of charge transfer where d.c. conductivity alone does not provide.

EXPERIMENTAL

Samples Preparation

Pure Polyaniline powder was purchased from Aldrich and was stored under nitrogen atmosphere. Five equal weights of 0.20 g of the pure polyaniline (Emeraldine base EB) were externally protonated in 5 different sulfuric acids of molarities 0.05, 0.07, 0.10, 0.15, and 0.20 molar. Each sample was kept in the acidic solution for 30 min to obtain the Emeraldine salt; all salts were then washed with distilled water several times. Prior to washing, each salt was centrifuged for several minutes. The samples were dried in an oven at a temperature of 80°C under nitrogen atmosphere. The doped polyaniline powder was pressed under 10 tons/cm^2 for 10 min forming circular discs of 13 mm in diameter and with thickness ranging from 0.5 mm to 0.7 mm.

X-Ray Diffraction

Powder X-ray diffraction (XRD) was performed using a PW 1729 Philips diffractometer interfaced with a computer control unit model PW1710 using copper source (K_α radiation, $\lambda = 1.54\,\text{Å}$). The angular range of 2θ was between 3° and 80° because no peaks were observed below 3° for all samples. The scanning speed of the diffractometer was 0.02°–0.04° (2θ/s) depending on the quality of signal-to-noise ratio. The positions of the peaks were determined by curve-fitting procedure of the experimental XRD data using Table Curve-2D software (Lowess Algorithm).

Thermal Measurements

The thermogravimetric analysis (TGA) and differential scanning calorimetry (DSC) were recorded using Shimadzu TGA-50 and DSC-50,

respectively, under nitrogen atmosphere in the temperature range of 30°C to 150°C and with a heating rate of 10°C/minute.

A.C. Measurements

Samples of Polyaniline doped with different concentrations of H_2SO_4, about 0.15 g of very fine powder was compressed at 10 ton.cm^{-2} for 10 min forming circular discs 13 mm in diameter and varied thickness between 0.5 to 0.7 mm. A silver coating was applied to each surface of the disc. It was then sandwiched between two brass circular discs to ensure good ohmic contacts with brass electrodes. The a.c. measurements were performed in the frequency range between 1 Hz and 10^6 Hz and in the temperature range 25 up to 80°C using a 1260 Impedance Gain Phase Analyzer (Solarton Analytical). The system was controlled using the Z–60 and Z-View Packages, which maximize the performance and data handling of the system. The generator amplitude was kept at 0.5 rms volts and zero d.c. bias. The complex a.c. impedance and the phase angle were measured, whereas the real and imaginary components of dielectric constant, impedance, and electric modulus were calculated [22].

RESULTS AND DISCUSSION

Figure 2 displays the XRD profiles of the three protonated PANI samples together with the pure PANI sample. The XRD pattern of sample (S_1) protonated with 0.1 M H_2SO_4 acid consists of one broad peak with an average area 5490 units. It has three additional peaks on the middle of the broad peak positioned at $2\theta = 21.6$, 24.4, and 25.6 degrees [23–25]. This reveals that the polymer matrix is amorphous in nature. The average position of the extra peaks was calculated using Bragg's law ($2d \sin(\theta) = n\lambda$) with $\lambda_{cu} = 1.54$ Å and found to be: 4.109 Å, 3.644 Å and 3.475 Å, respectively.

The XRD pattern for sample S_2, protonated with 0.15 M H_2SO_4 acid consists of four extra peaks on the main broad one, using Bragg's law, the position of each peak was calculated and found to be: d = 4.25 Å, 3.964 Å, 3.797 Å, and 3.530 Å. The XRD pattern for sample S_3 protonated with 0.2 M H_2SO_4 acid consists of two broad peaks. The first broad peak centered at $2\theta = 12$ degrees, whereas the second peak has two extra sharp peaks centered at $2\theta = 23.2^\circ$ and 25.15°. The calculated positions of these peaks are found to be d = 7.366 Å, 3.830 Å, and 3.537 Å. Close inspection of these positions shows that they are slightly shifted toward higher chain–chain separation. The observation that

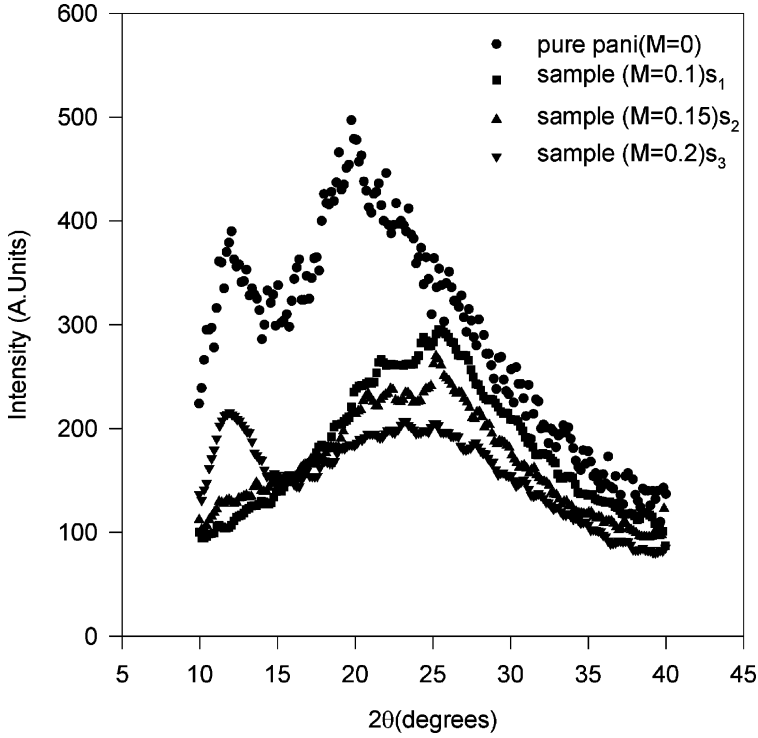

FIGURE 2 The X-ray diffraction intensity versus diffraction angle (2θ) for pure and doped samples of PANI.

the chain separation has slightly increased with the increase of degree of doping demonstrates that a gradual change in the internal structure of the polymer has happened, which suggests that the PANI chain became bent at the anion site (see Figure 1). This leads to an off plane rotation that tends to increase the separation between the σ bonds, resulting in lowering the possibility of electron hopping from one site to another. Such a mechanism gives rise to insulator metal transition [23–25].

Figure 3 displays the normalized (TGA) profiles for pure PANI sample together with the three protonated samples S_1, S_2, and S_3. It is clear that the weight loss in the temperature range from room temperature up to 80°C is less than 0.06%. This weight loss cannot explain the large variations in the values of the bulk resistance with temperature or those obtained from the a.c. measurements. Figure 3 indicates the occurrence of the transition in the TGA at doping concentration 0.15 M and above.

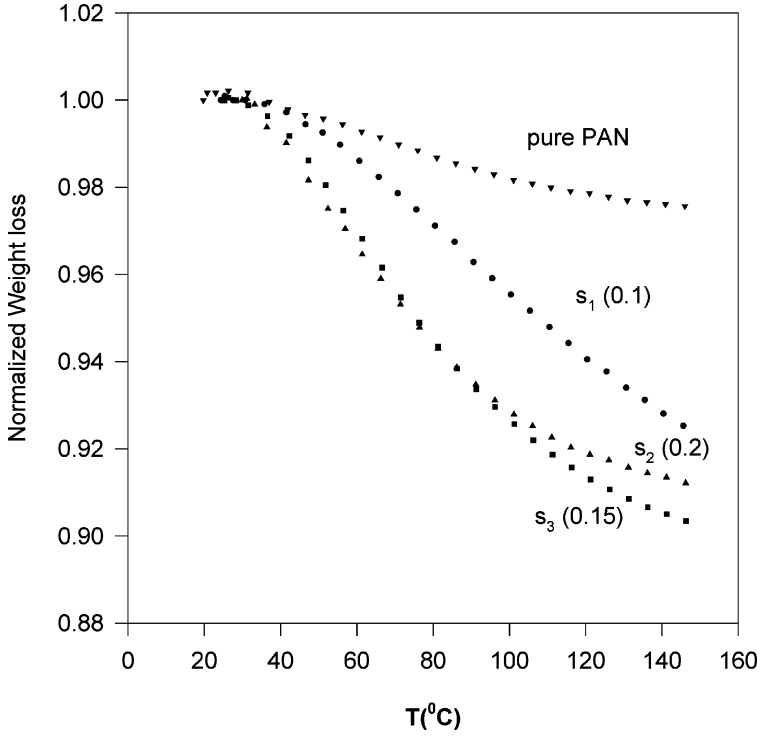

FIGURE 3 Normalized weight loss versus temperature (°C) for pure and doped PANI.

Figure 4 displays the DSC data for the same samples (S_1, S_2, and S_3). It is clear that pure PANI suffers no phase change within the temperature range of interest, and the sharp decrease in the absorbed power is due to water adsorbed to the surface of the polyaniline. Samples S_1, S_2, and S_3 are endothermic with a slight shift in the position of the absorption minimum toward higher temperatures. The sharp absorption minimum seen in sample S_2 is associated with the structural change seen in the XRD data.

On the other hand, studying a.c. electrical properties of materials may provide valuable information about the conduction mechanisms occurring in polymers and macromolecular metal complexes, which may involve electronic, ionic interfacial, and space charge polarization. The magnitude of the effects may be understood from the behavior of the real and imaginary components of dielectric constants, a.c. impedance, and electric modulus. At any particular frequency, the complex

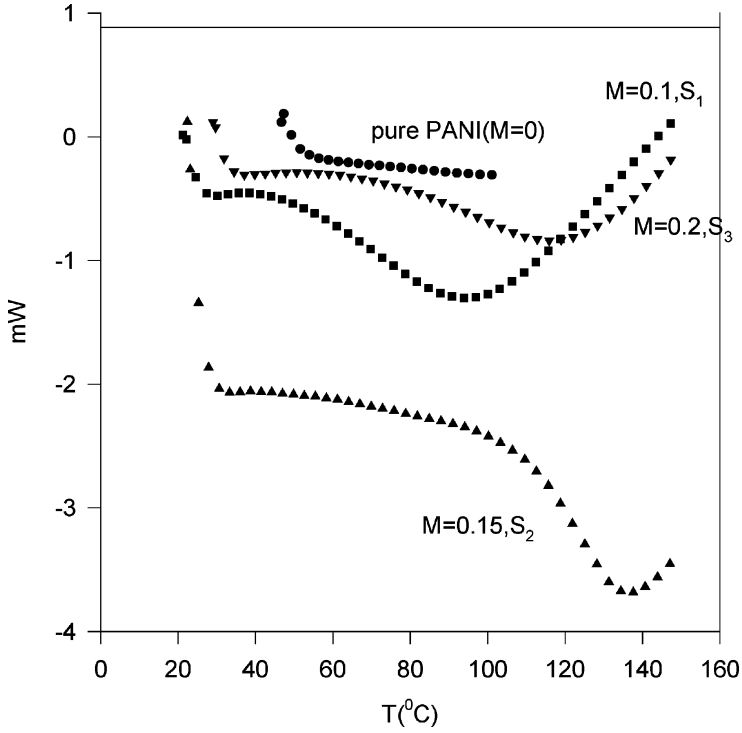

FIGURE 4 Absorbed heat (mW) versus temperature for pure and doped PANI.

impedance Z^* and the complex dielectric constant ϵ^* are expressed in terms of their real and imaginary components, respectively:

$$Z^* = Z' - iZ'' \quad \text{and} \quad \epsilon^* = \epsilon' - i\epsilon''$$

where, Z', ϵ' are the real components and Z'', ϵ'' are the imaginary components of the a.c. impedance and dielectric constant, respectively. The relationships between the dielectric constants and a.c. impedance are:

$$\epsilon' = Z''/2\pi f C_0 Z^2$$

$$\epsilon'' = Z'/2\pi f C_0 Z^2$$

where C_0 is the capacitance of the electrodes.

On the other hand, an electrical modulus M^* is used in the literature [26], which is related to the dielectric constant by the relation:

$$M^* = (\epsilon^*)^{-1} = M' - iM''$$

where M′ is the real component

$$= \frac{\epsilon'}{(\epsilon'^2 + \epsilon''^2)}$$

and M″ is the imaginary component

$$= \frac{\epsilon''}{(\epsilon'^2 + \epsilon''^2)}$$

Figure 5 (a and c) show the variation of Z′ versus frequency as a function of temperature for a PANI sample protonated in 0.05 and 0.2 molar H_2SO_4 acid, respectively. These figures show 3 main features, in the first region from 1 Hz to 10^3 Hz; Z′ varies very slowly with frequency, indicating that the resistive type behavior is more dominant. In the second region (10^3 to 10^6 Hz) a high frequency fall-off of Z′ as f^{-1}, which is due to capacitive effects within the system from cables, physical geometry of the contacts, and the input capacitance of the measurements equipment. The third feature is the decrease in Z′ with increasing temperature for 0.05 M sample (Figure 5a), similar to that observed in many polymers [27]. However, for 0.2 M sample Z′ increases with increasing temperature indicating that an insulator metal (I-M) transition took place with increasing the doping of the samples. The I-M transition has been observed for different polymers such as polyacetylene, polypyrrole, and polyaniline [28–31]. It was reported that in the metallic and insulator regimes the plot of $\ln \Delta\sigma/\Delta T$ versus T exhibits a positive and negative temperature coefficients for insulator to metal transition, respectively, where the transport in insulating regime occurs through wide range hopping among localized states. On the other hand, the plot of the imaginary component of complex impedance, as shown in Figures 5 (b and d), shows in both samples well-defined relaxation peaks. However, the intensity of such peaks for 0.05 M sample decreases and moves to higher frequency with increasing temperature, whereas for 0.2 M sample the intensity of the relaxation peaks increases with increasing temperature and moves to a lower temperature, supporting the concept of Insulator to metal transition. However, the Cole-Cole plot of (Z′ versus Z″) as shown in Figure 6 (a and b) consists of a depressed, slightly distorted, semicircle at temperature 30°C, which becomes a nearly perfect semicircle with increasing temperature for 0.02 M sample, with slightly distorted semicircles observed even at high temperature. The semicircle corresponds to a parallel combination of a nondispersive d.c. conductance and a slightly dispersive capacitance. The radius of Cole-Cole plot, which represents the bulk resistance of the sample under test, shows a decrease with increasing temperature for the

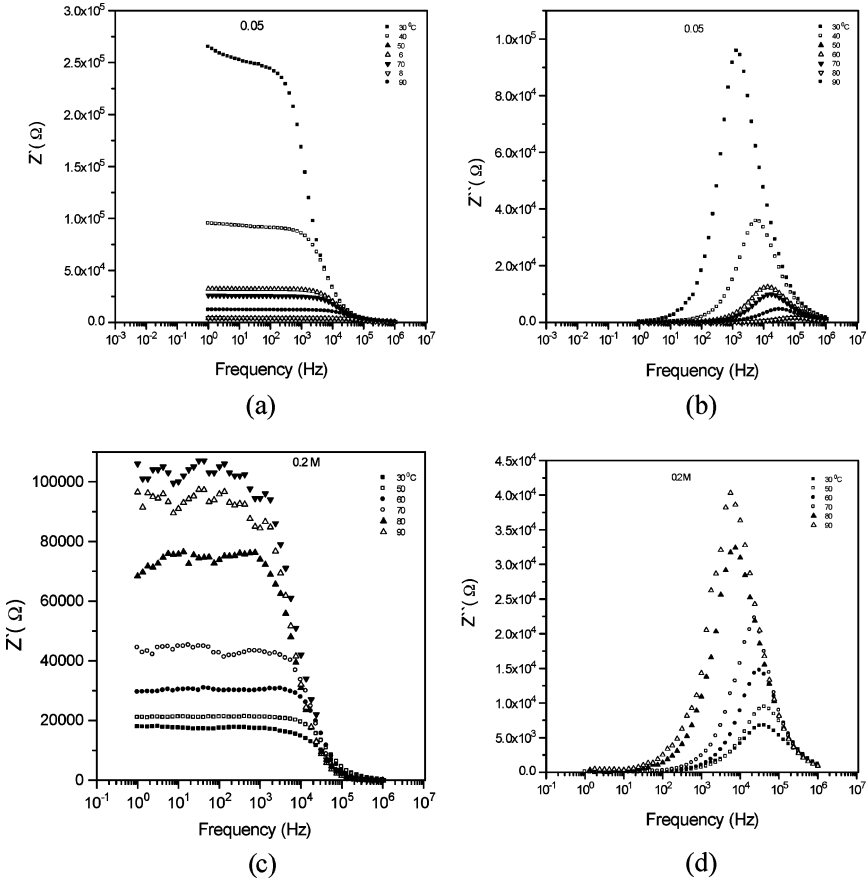

FIGURE 5 Real (Z′) and imaginary (Z″) component of complex impedance versus frequency for doped PANI at different temperature. (a) and (b) for M = 0.05, (c) and (d) for M = 0.2.

0.05 M sample although an increase in the bulk resistance was observed with increasing temperature for 0.2 M sample. The conductivity of the samples can be determined from the Cole-Cole plot, where the diameter of the semicircle represents the bulk resistance, where,

$$\sigma = \frac{\mathrm{d}}{\mathrm{RA}}$$

where d is the sample thickness, A is the cross-sectional area, and R is the bulk resistance. On the other hand, the relaxation time ($\tau = 1/2\,\pi \mathrm{f}_{\max}$) was determined from Cole-Cole plot. The results of conductivity and

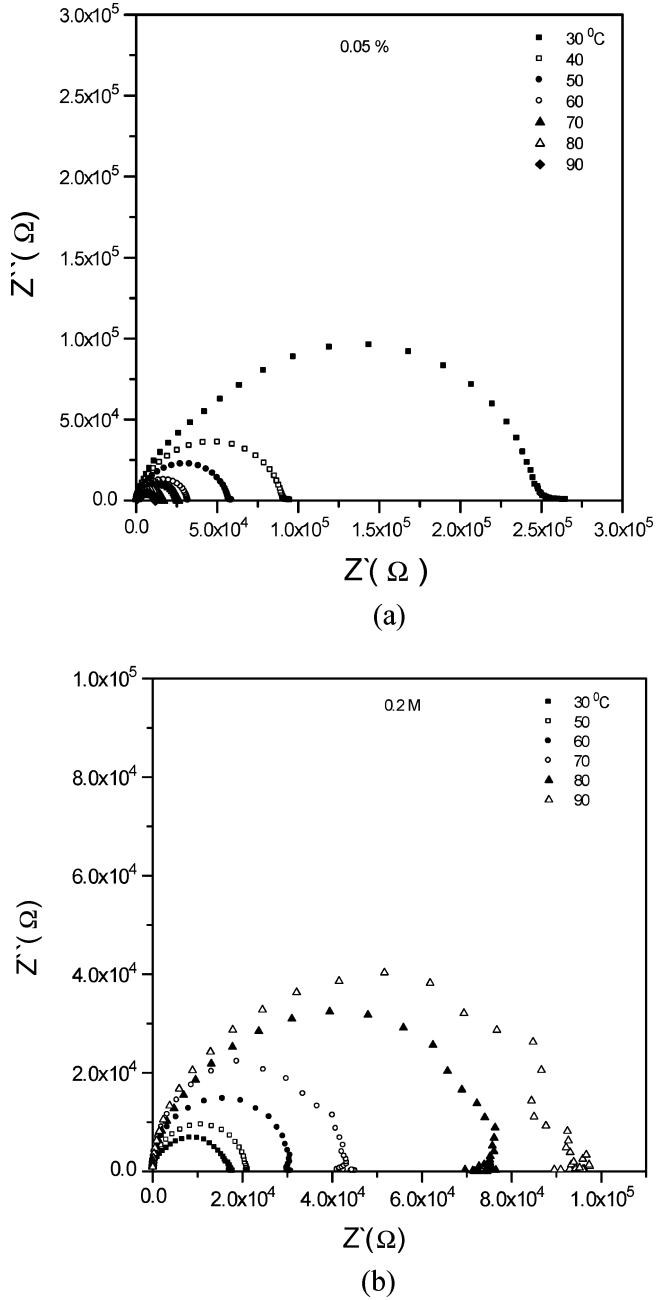

FIGURE 6 Z′ versus Z″ for doped PANI at different temperature. (a) for M = 0.05. (b) for M = 0.2.

relaxation time plotted versus 1/T are shown in Figure 7 (a and b). The difference in the relaxation time with temperature may be due to the electric charges displaced inside the polymer structure (storage localization). The calculated activation energy for 0.05 sample is in the order of 39.9×10^3 kJ/kmole (0.414 eV/molecule) and decreases to 13.2×10^3 kJ/kmole (0.14 eV/molecule). For higher doping concentration a positive slope was observed indicating that the ordered mesoscopic regions in highly doped samples are more metallic with respect to that of low doping. It seems that upon doping in 0.2 M the mid-gap polaronic state level broadens and merges with conduction/valence bands and this induces the transition from insulator to metal.

The relaxation time, as well as conductivity for PANI samples versus temperature, shows an insulator to metal transition at concentrations greater than 0.1 M. Such a transition may be due to the internal change in the structure of the polymer and to the off plane rotation in the chain at the anion site, as seen in the XRD data.

However, both conduction mechanism and electronic plus ionic are operative in this system as seen from the tail in the Z′ versus Z″ plots. Nevertheless, from the values of activation energies, it is reasonable to conclude that the conduction mechanism in protonated PANI system is electronic in nature rather than ionic. However, the ionic conduction can not be excluded from electronic conduction, which is nearly dominant in doped PANI system.

The dependence of relative permittivity (ϵ') and the dielectric loss ϵ'' on frequency for doped samples is shown in Figure 8 (a and b). ϵ' is minimum in the frequency range higher than 10^4 Hz for a sample containing 0.05 M. However, at low frequency a sharp increase in ϵ' was observed in the samples containing 0.1 and 0.2 M indicating that the ionic conduction is more dominant in these samples. The log plot for dielectric loss yield a straight line in the frequency less than 10^5 Hz. The dependence of relative permittivity on temperature for doped samples 0.05 M and 0.2 M are shown in Figure 9. Two main features were observed. First no relaxation peak appears in the plot of the loss factor ϵ''. It is believed that the ionic conduction in the low frequency region may mask any relaxation. Therefore, to analyze the conductivity relaxation process, the complex permittivity is converted to the complex electric modulus M* according to the following relations:

$$\mathrm{M}' = \frac{\epsilon''}{\epsilon'^2 + \epsilon''^2}$$

$$\mathrm{M}'' = \frac{\epsilon''^2}{\epsilon'^2 + \epsilon''^2}$$

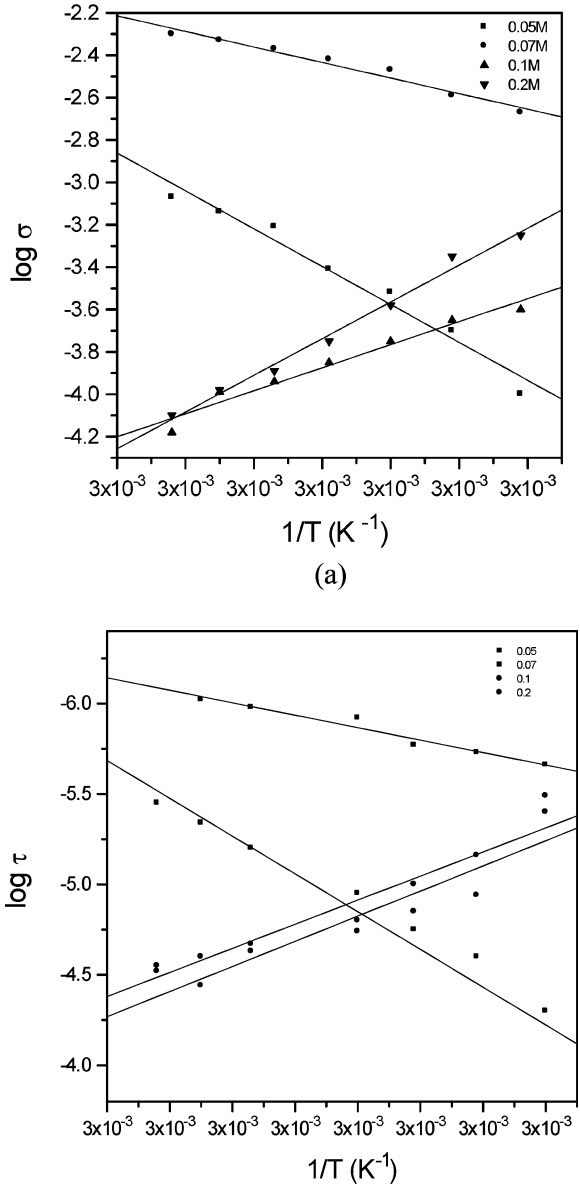

FIGURE 7 (a) log a.c. conductivity ($\Omega \cdot \text{cm}^{-1}$) and (b) log relaxation time for doped PANI samples.

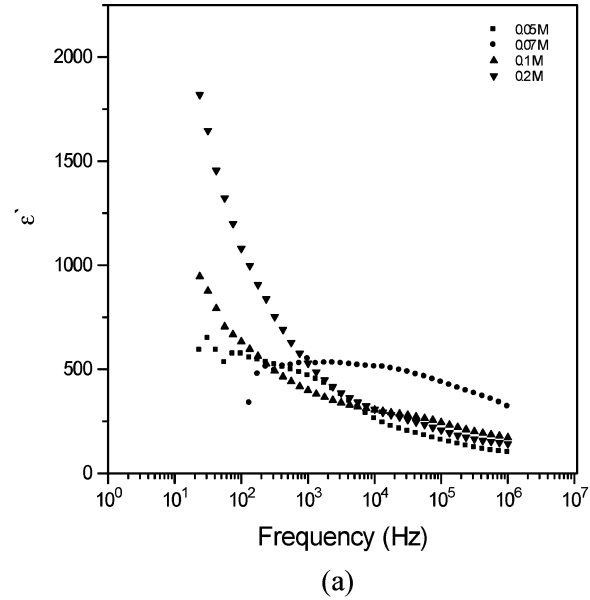

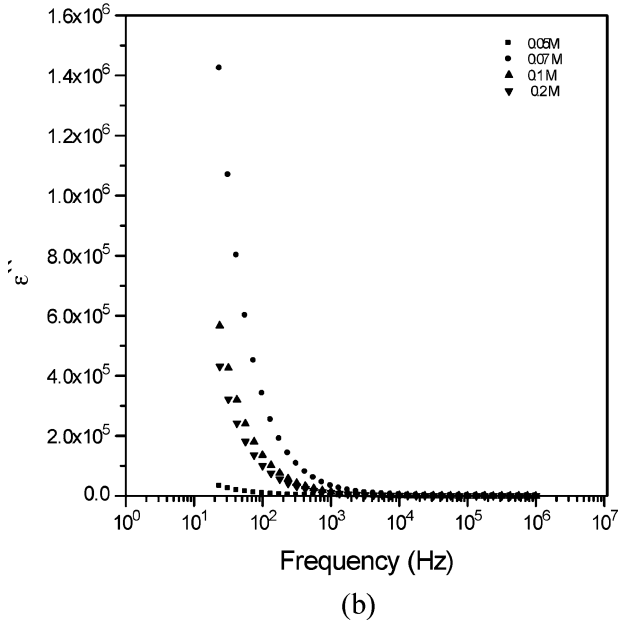

FIGURE 8 (a) Relative permittivity (ϵ') and (b) dielectric loss (ϵ'') versus frequency for doped PANI samples.

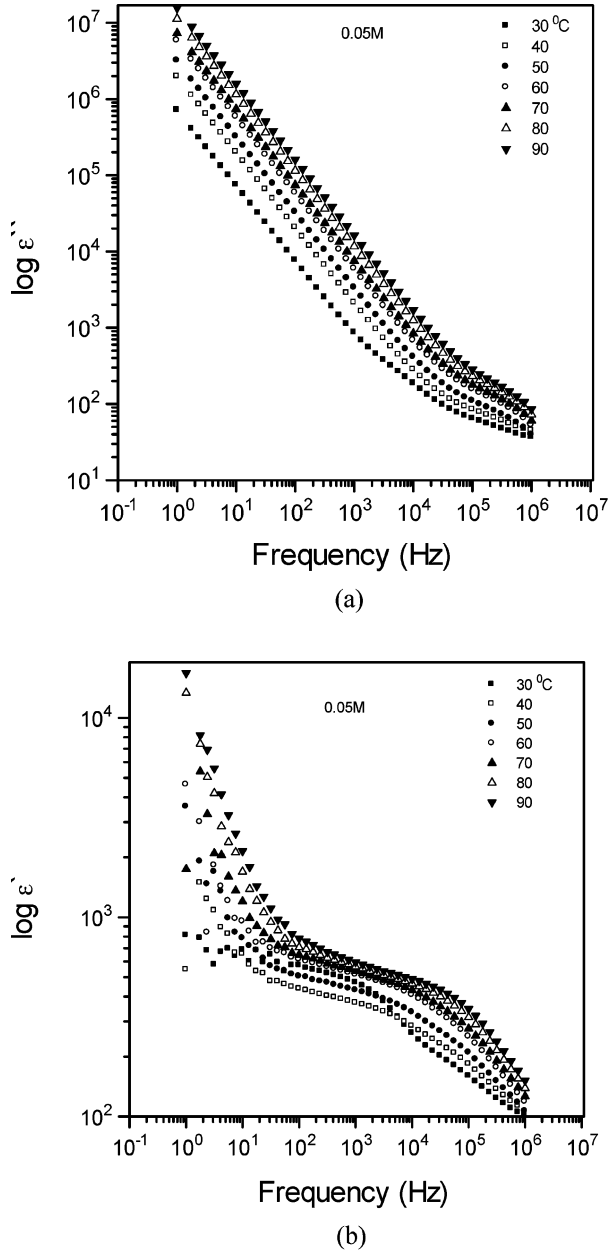

FIGURE 9 (a) $\log \epsilon'$ versus frequency for M = 0.05. (b) $\log \epsilon''$ versus frequency for M = 0.2 for doped PANI samples.

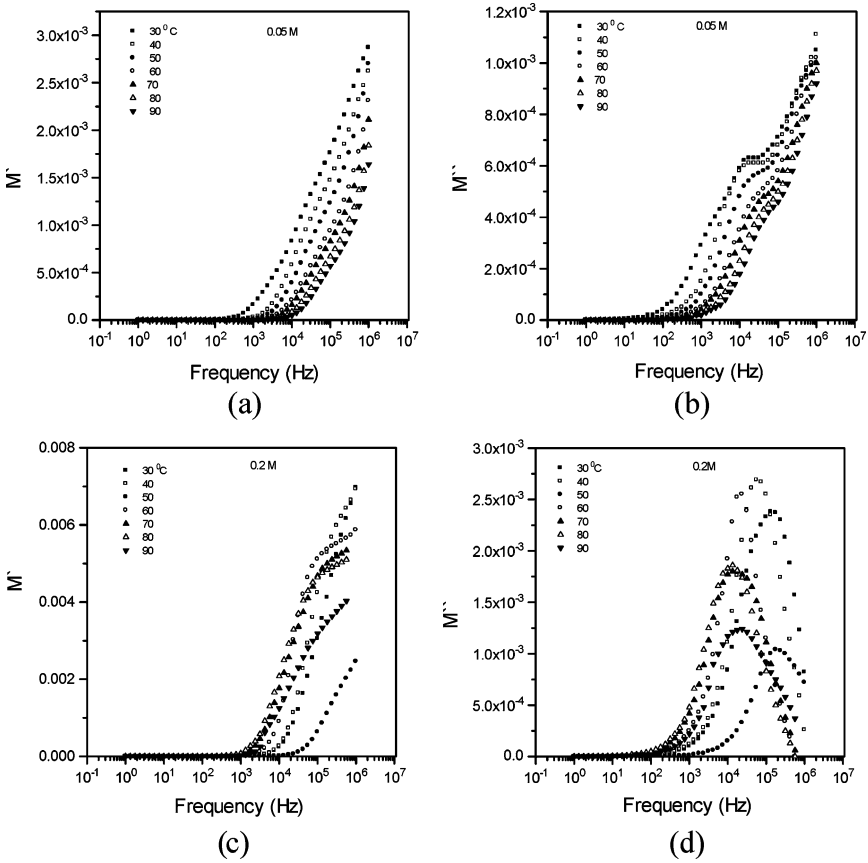

FIGURE 10 Real (M′) and imaginary (M″) components of complex modulus versus frequency for doped PANI samples.

In these relations, ϵ' appears in the denominator to the second power and its tendency to overwhelm the loss factor is minimized. In addition the electric modulus is especially useful for analyzing electrical relaxation processes whose measurements are compromised by high capacitance effects, such as those due to inter-granular impedance and electrode polarization. This advantage rests in the fact that any capacitance in series with an arbitrary impedance adds a constant to M′ but does not affect M″. Therefore, if an undesirable capacitance occurs in series with element of an equivalent circuit, rather than in series with the circuit itself, M″ can also sometimes suppress its effects if the capacitance is large compared with other capacitances in the circuit.

From the dependence of M′ and M″ on frequency as shown in Figure 10, the dispersion of M′ and M″ indicate the presence of relaxation time distribution of conduction. However, the relaxation peaks in 0.2 M sample is more defined than that in 0.05 M. In Figure 10 (a and c), M′ approaches zero at low frequencies indicating that the electrode polarization gives a negligible low contribution to M′ and can be ignored. The maximum peak in M″ decreases in intensity and moves to higher frequency with increasing temperature for the 0.05 M sample. This coincides well with the results of Lee et al. [32], who found that in doped polymers, the peak shifts toward higher frequencies with increasing d.c. conductivity.

The plot of log loss factor versus temperature for 0.05 M and 0.2 M samples is shown in Figure 11 (b and d) a straight line with a slope nearly 1 was observed in the frequency range 1 Hz to about 10^5 Hz, for both samples as a function of temperature, that is

$$\text{Log } \epsilon'' \alpha \, f^{-1}.$$

CONCLUSIONS

The electrical, thermal, and structural properties of conducting PANI depend on the method of preparations and on the degree of doping as well as on the type of acid used. Samples doped in relatively high concentrations show metal to insulator transition, a mechanism that needs more research and study. The study shows that electron hopping is the dominant type of conduction.

REFERENCES

[1] MacDiarmid, A. G. and Epstein, A. J., *Faraday Discuss. Chem. Soc.* **88**, 317 (1989).
[2] Stejskal, J. and Kratochvil, P., *Polymer* **37**, 367 (1996).
[3] Trivedi, D. C. (1997). In *Handbook of Organic Conductive Molecules and Polymers*. H. S. Nalwa, Ed., Vol. 2, Wiley, Chichester, pp. 505–572.
[4] Gospodinova, N. and Terlemezyan, L., *Prog. Polym. Sci.* **23**, 1443 (1998).
[5] Levi, B. G., *Phys. Today* **53**, 19 (2000).
[6] MacDiarmid, A. G., *Angew, Chem. Int. Ed.* **40**, 2581 (2001).
[7] Jin, Z. and Duan, Y., *Sens. Actuators B* **72**, 75 (2001).
[8] Sotomayor, P. T., Raimundo, I. M., Jr., Zarbin, A. J. G., Rohwedder, J. J. R., Netto, G. O., and Alves, O. L., *Sens. Actuators B* **74**, 157 (2001).
[9] Kane, L. A. P., Maguire, S., and Allace, G. G., *Synth. Met.* **119**, 39 (2001).
[10] Hamers, R. J., *Nature* **412**, 489 (2001).
[11] Rosseinsky, D. R. and Ortimer, R. J., *Adv. Mater.* **13**, 783 (2001).
[12] Prokes, J., Krivka, I., Tobolkova, E., and Stejskal, J., *Polym. Degrad. Stab.* **68**, 261 (2001).
[13] Elyashevich, G. K., Terlemezyan, L., Kuryndin, I. S., Lavrentyev, V. K., Mokreva, P., Rosova, E. Yu., and Sazanov, Y. N., *Thermochim. Acta* **374**, 23 (2001).

[14] El-Sherif, M. A., Yuan, J., and MacDiarmid, A. G., *J. Intelligent Mater. Syst. Struct.* **11**, 407 (2001).
[15] Stejskal, J., Hlavata, D., Holler, P., Trchova, M., Prokes, J., and Sapurina, I., *Polym. Int.* **53**, 300 (2004).
[16] Zuo, F., Angelopoulos, M., MacDiarmid, A. G., and Epstein, A. J., *Phys. Rev. B* **39**, 3570 (1989).
[17] Javadi, H. H. S., Cromack, K. R., MacDiarmid, A. G., and Epstein, A. J., *Phys. Rev. B* **39**, 3579 (1989).
[18] Lux, F., *Polymer* **35**, 2915 (1994).
[19] Regbu, M., Cao, Y., Moses, D., and Heeger, A. J., *Phys. Rev. B* **47**, 1758 (1993).
[20] Kahol, P. K., Pinto, N. J., Berndtsson, E. J., and McCormick, B. J., *J. Phys. Condens. Matter* **6**, 5631 (1994).
[21] Kivelson, S., *Phys. Rev. B* **25**, 3798 (1982).
[22] El Ghanem, H. M., Abdul Jawad, S., Aljundi, J., Afaneh, F., and Arafa, I., *Poly. Int.* **52**, 1125 (2003).
[23] Wan, M., Li, M., and Liu, Z., *J. Appl. Polym Sci.* **3**, 131 (1994).
[24] Wan, M. and Li, J., *J Polym. Sci. A* **36**, 2799 (1998).
[25] Rajendra, K. and Munichand, N., *Synthe. Met.* **17**, 130 (2003).
[26] Haward, W., Starkwether, J. R., and Avakian, P., *J Polym. Sci. Phys. Ed.* **30**, 637 (1992).
[27] Hodge, I. M., Ingram, M. D., and West, R. J., *J. Electroanal. Chem.* **74**, 125 (1976).
[28] Al Dujaili, A., Shalash, R., and Yasagh, T., *Eur. Polym. J.* **29**, 974 (1990).
[29] Macedo, P. B., Magniham, C. T., and Bose, R., *Phys. Chem. Glasses* **13**, 71 (1971).
[30] Menson, R., Yoan, C. O., Moses, D., and Heeger, A. J. (1998). In *Handbook of Conducting Polymers*. Second Edition, T. A. Skothein, R. L. Elsenbaumer, and J. R. Reynolds, Eds., Marcel Dekker, Inc., New York, pp. 937–1039.
[31] Zabrodskii, A. G. and Zinavjeva, K. N., *Zh. EKSP. Teor. Fiz.* **86**, 727 (1984).
[32] Lee, H., Liao, C. S., and Chen, S. A., *Makromol. Chem.* **194**, 2443 (1993).